Polym. Bull. (2010) 64:245–257
DOI 10.1007/s00289-009-0159-3

ORIGINAL PAPER

SBS nanocomposites as toughening agent for polypropylene

Patrícia A. da Silva · Marly M. Jacobi · Luciane K. Schneider · Ronilson V. Barbosa · Paulo A. Coutinho · Ricardo V. B. Oliveira · Raquel S. Mauler

Received: 16 June 2009 / Revised: 4 August 2009 / Accepted: 6 September 2009 /
Published online: 18 September 2009

Abstract The toughening of polypropylene [PP] with styrene–butadiene–styrene rubber [SBS]/montmorillonite [MMT] nanocomposites was investigated with respect to morphological, thermal, and mechanical properties. The MMT/SBS nanocomposites were prepared in an internal mixer, using an epoxidized SBS [SBSe] to investigate its effect as a compatibilizer. The MMT/SBS nanocomposite was added to PP up to 10 wt%, aiming at material toughening. Transmission electron microscopy (TEM) revealed MMT induced dispersed-phase reductions when compared to typical PP/SBS blends. In addition, changes in the PP crystallization process were observed in the presence of the nanocomposite. Surprisingly, the use of nanofiller, combined with SBSe compatibilizer agent, increased the PP impact strength by about 60%, with no reduction in the tensile module.

Keywords Nanocomposite · SBS · Blends · Toughening agent · Morphology

Introduction

Polypropylene [PP] is quite an outstanding polymeric material with respect to its performance, in particular, to its wide property spectrum, easy processability,

P. A. da Silva · M. M. Jacobi · L. K. Schneider · R. V. B. Oliveira (✉) · R. S. Mauler
Instituto de Química, Universidade Federal do Rio Grande do Sul (UFRGS), Av. Bento Gonçalves, Porto Alegre, RS 9500, Brazil
e-mail: ricardo.oliveira@iq.ufrgs.br

R. V. Barbosa
Instituto de Química, Universidade Federal do Paraná (UFPR), Rua XV de novembro, Curitiba, PR 1299, Brazil

P. A. Coutinho
Braskem S/A, Triunfo, RS, Brazil

versatility of applications, and attractive combination of favorable economic conditions [1]. However, its application as an engineering thermoplastic is somewhat limited because of its relatively poor impact strength, especially at low temperatures [2, 3]. In order to improve impact toughness of the PP, it is common practice to incorporate elastomers, but its stiffness and tensile strength are thus simultaneously reduced. Several elastomers, which had been studied with this purpose among others, are polyisobutylene, styrene–butadiene copolymer, and ethylene–propylene copolymers.

Otherwise, polymer-layered silicate nanocomposites have attracted a great deal of interest over the past few years as a result of the potentially superior properties that these materials could exhibit relative to conventional composites [3–7]. Polymer-layered silicate nanocomposites contain low levels of dispersed mineral platelets with at least one dimension in the nanometer range. The most common mineral used is the montmorillonite [MMT] [8, 9]. However, it exhibits hydrophilic characteristics, and in order to increase its organophilicity, its surface can be modified with a quaternary alkylammmonium cations to expand its gallery spacing, and its affinity with polymer matrix. Normally, nonpolar polymers must be functionalized with polar functional groups to improve the compatibility between the polymer matrix and silicate clays [10, 11]. Nanocomposites present great advantages in relation to the neat polymer, such as the increase in modulus, tensile strength, and temperature of thermal distortion without significant increase in the material density [12, 13].

Recently, several authors have reported that clays can effectively reduce the domain size in polymer blends and that they play a role as compatibilizer in various immiscible polymer blends [14–17]. Most of them attributed this behavior to the ability of the compatibilizers to affect both the interfacial tension and the viscosity ratio, which are important factors in the determination of the size of the dispersed phase during melt mixing [18–22]. The compatibility between the phases of a blend can be improved by the addition of compatibilizers, which results in a finer and more stable morphology, better adhesion between the phases of the blends, and consequently better properties of the final product [23].

In this study, the influence of MMT addition to styrene–butadiene–styrene rubber [SBS] on the preparation of PP/SBS blends was evaluated concerning morphological, thermal, and mechanical properties. Besides, the use of an epoxidized SBS as compatibilizer was also considered.

Experimental

Materials

Polypropylene [PP] (MFI = 2.1 g 10^{-1} min^{-1}), kindly gifted by Braskem S/A, was used as polymeric matrix. The triblock styrene–butadiene–styrene rubber [SBS] (30 wt% of styrene, M_w = 73,000 g mol^{-1}, polydispersity 1.23) was provided by Petroflex S/A. The nanofiller used in this study was the MMT Cloisite 10 A (Southern Clay Products Co.), with organophilic modifier, dimethyl benzyl

hydrogenated tallow quaternary ammonium chloride. SBS with 15 mol% of epoxidized butadiene units [SBSe] ($M_w = 83{,}000$ g mol^{-1}, polydispersity 1.24) was used as compatibilizer between the MMT and neat SBS. The epoxidation was carried out in our laboratory using in situ-generated performic acid, as described elsewhere [24]. The epoxidation degree was determined by ^{1}H-NMR.

Melt processing

SBS/MMT nanocomposites [SBSn] (3 wt% of MMT) were produced in a Haake Rheomix 600 mixer, at 60 RPM, 130 °C, during 5 min after loading. SBS nanocomposites containing epoxidized rubber [SBSne] were prepared as described elsewhere [25]. The rubber nanocomposites were compression-molded at 160 °C, cooled, grained, and then blended with PP at 60 RPM, 180 °C, for 7 min. Table 1 presents the compositions of the PP/SBS, PP/SBSn, and PP/SBSne blends.

Morphological studies

Morphological studies were examined by scanning electron microscopy [SEM], using a JEOL model JSM 6060 microscopy. The samples were fractured in liquid nitrogen to avoid any phase deformation during cracking process. The rubber phase was preferentially extracted by immersing the fractured surface in tetrahydrofuran (THF) for 4 h. The samples were later dried in vacuum oven at 40 °C for 3 h for solvent elimination. The dispersion and morphology of the MMT nanoparticles in the blends were also analyzed by transmission electron microscopy [TEM] (JEOL model JEM 1200 ExII) with an accelerating voltage of 80 kV. Samples were prepared by means of a cryo-ultramicrotome using a diamond knife. In TEM micrographs, dispersed-phase droplets (at least 30) were detected and analyzed through Imagetool version 3.0 software.

Mechanical testing

The specimens were obtained by compression molding (180 °C, 14 min, 4 lbf), in the shape of tensile dog bones, using a modified ASTM D 638 standard (sample thickness of 1.5 mm). Tensile tests were performed using an EMIC model DL10000

Table 1 Compositions of PP/SBS systems

System	PP/SBS/MMT/SBSe (wt%)
PP	100/0/0/0
PP/SBS$_5$	95/5/0/0
PP/SBS$_{10}$	90/10/0/0
PP/SBSn$_5$	95/4.85/0.15/0
PP/SBSn$_{10}$	90/9.70/0.30/0
PP/SBSne$_5$	95/4.60/0.15/0.25
PP/SBSne$_{10}$	90/9.20/0.30/0.50

at a cross-head speed of 50 mm/min at room temperature. Notched Izod impact tests were performed also at room temperature using an Emic Izod pendulum (6.8 J hammer and 3.5 m s^{-1} impact velocity) according to ASTM D256 standard. All the samples were acclimatized for at least 24 h prior to tests.

Differential scanning calorimetry (DSC)

DSC experiments were carried out in a DSC Thermal Analyst 2100/TA Instrument from 50 to 200 °C. The samples (6–8 mg) were heated and cooled at a scanning rate of 10 °C min^{-1} under nitrogen atmosphere (50 mL min^{-1}) to avoid oxidation. To calculate the crystallinity of PP, a value of melting enthalpy of 190 J g^{-1} was used [26].

Results and discussion

Blends morphologies

The Fig. 1a–f presents the SEM micrographs of PP/SBS, PP/SBSn, and PP/SBSne blends. As expected, the increase of rubber content from 5 (Fig. 1a, c, e) to 10 wt% (Fig. 1b, d, f) in the PP blends induced increases in the domains sizes for all the systems, even in the presence of MMT or SBSe. The morphology of a polymer blend possesses a dynamic character, i.e. changes over time, as a result of the equilibrium between the break-up and coalescence of the dispersed/deformed domains in the matrix flow field [27]. In our case the increase in elastomeric phase encourages coalescence. Thus, coalescence occurs during processing at higher concentrations of the dispersed phase, resulting in the larger particle size [18, 27].

On the other hand, some authors [18, 28, 29] reported that the addition of a compatibilizer or nanofiller in the blend suppresses domains' coalescence, due to the stabilization of the interface and a reduction in the interfacial tension.

In our systems, the organoclay seems to act as a barrier to prevent coalescence of rubber domains and thus might cause the decrease of rubber particle size in the PP matrix. This behavior could be explained by the reduction of mass transfer between rubber domains through the influence of organoclay. Also, the use of SBSe as compatibilizer reduced the domains' sizes even more. The SBSe probably reduced the interfacial tension between phases, inducing a reduction in the domains' sizes, resulting in a more homogeneous morphology.

The nanocomposites of SBS were also analyzed by X-ray diffraction (Fig. 2). The principal MMT diffraction peak at 4.8° is related to a basal distance of *X* nm within platelets. When the organoclay was added to both SBS rubbers significant changes in diffraction pattern were detected. The MMT peak was shifted to 2.1°, and consequently the basal distance was augmented to *X* nm. These observations suggest SBS macromolecules may have penetrated into MMT galleries. Besides, the presence of epoxidized rubber SBSe appears to have no considerable influence on clay sheet spacing. Hence, further discussions on rubber nanocomposites morphologies will be addressed later in this article.

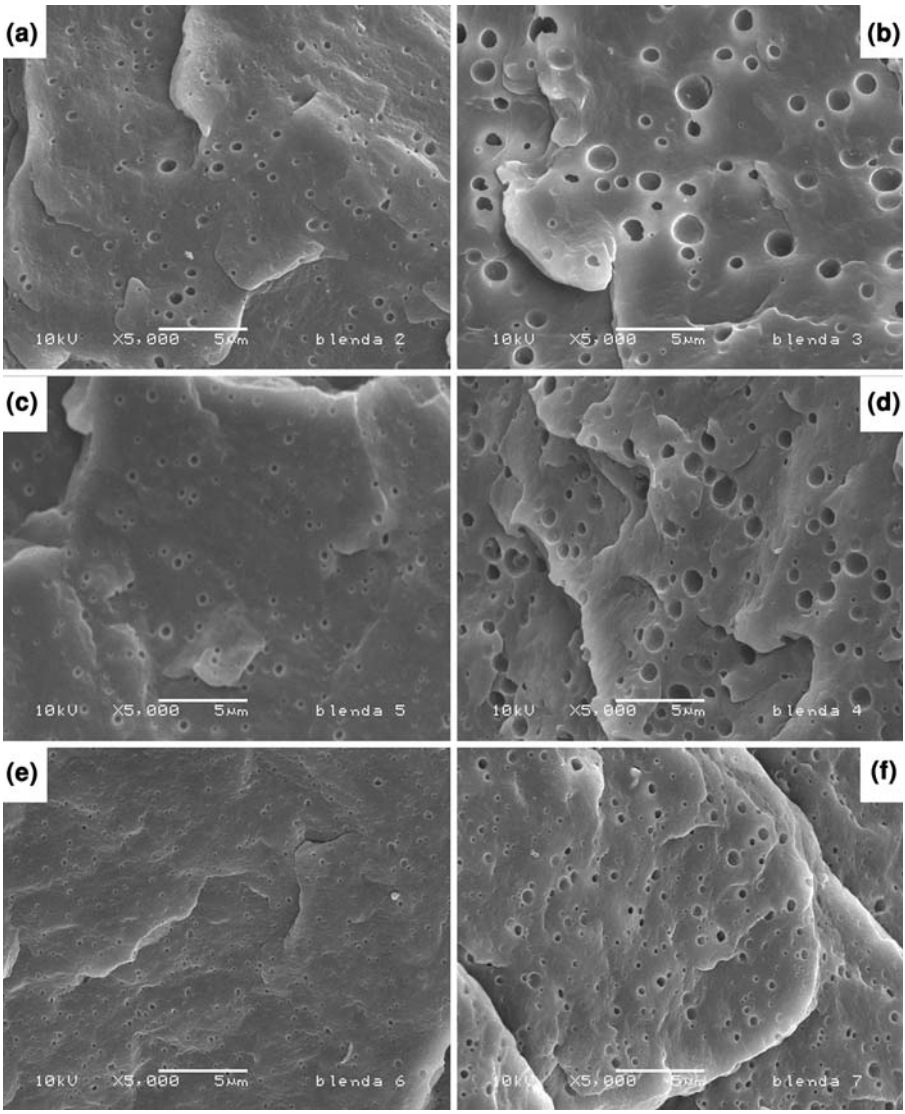

Fig. 1 SEM micrographs of **a** PP/SBS_5, **b** PP/SBS_{10}, **c** PP/$SBSn_5$, **d** PP/$SBSn_{10}$, **e** PP/$SBSne_5$, and **f** PP/$SBSne_{10}$ nanocomposites

Arroyo et al. noticed similar behavior in their study involving epoxidized natural rubber [12]. In addition, this compatibilizer probably improved the dispersion of MMT in the SBS, increasing the adhesion of the epoxidized rubber promoting in the clay exfoliation, as can be seen in Fig. 3.

Figure 4 presents the TEM micrographs of PP/SBS blends. As observed by SEM, the PP/SBS blend without clay presented the largest domains. The presence of MMT decreased the size of the rubber domains probably by increasing the

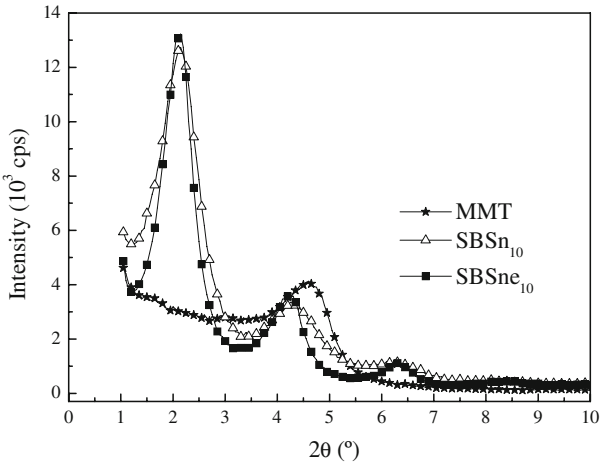

Fig. 2 XRD of MMT (*filled star*), SBSn$_{10}$(*open triangle*), and SBSne$_{10}$ (*filled square*) nanocomposites

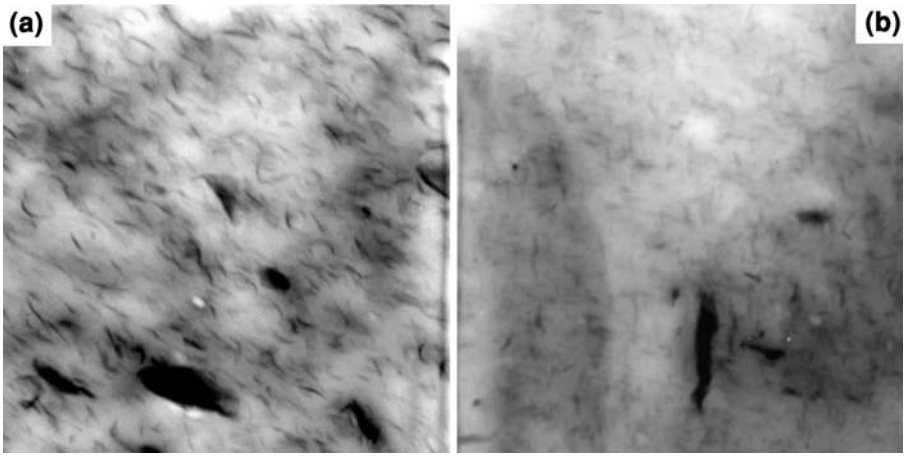

Fig. 3 TEM micrographs (width = 6 μm) of **a** SBSn$_{10}$ and **b** SBSne$_{10}$ nanocomposites

dispersed-phase melt viscosity which could, in turn, render the coalescence of rubber droplets difficult.

Moreover, the use of epoxidized rubber SBSe produced small changes in the domains' sizes. Interestingly, the compatibilizer induces the MMT to be preferentially placed at the interface between rubber and PP. Various authors [28, 30–33] also observed similar behavior. Kelnar et al. [32] observed a decrease in dispersed-phase size and the formation of "core–shell" particles, which seem to occur mainly as a consequence of simultaneous clay localization at the interface, representing the "true compatibilization effect" with expected co-intercalation and/or absorption of both polymers and clay in the interfacial region.

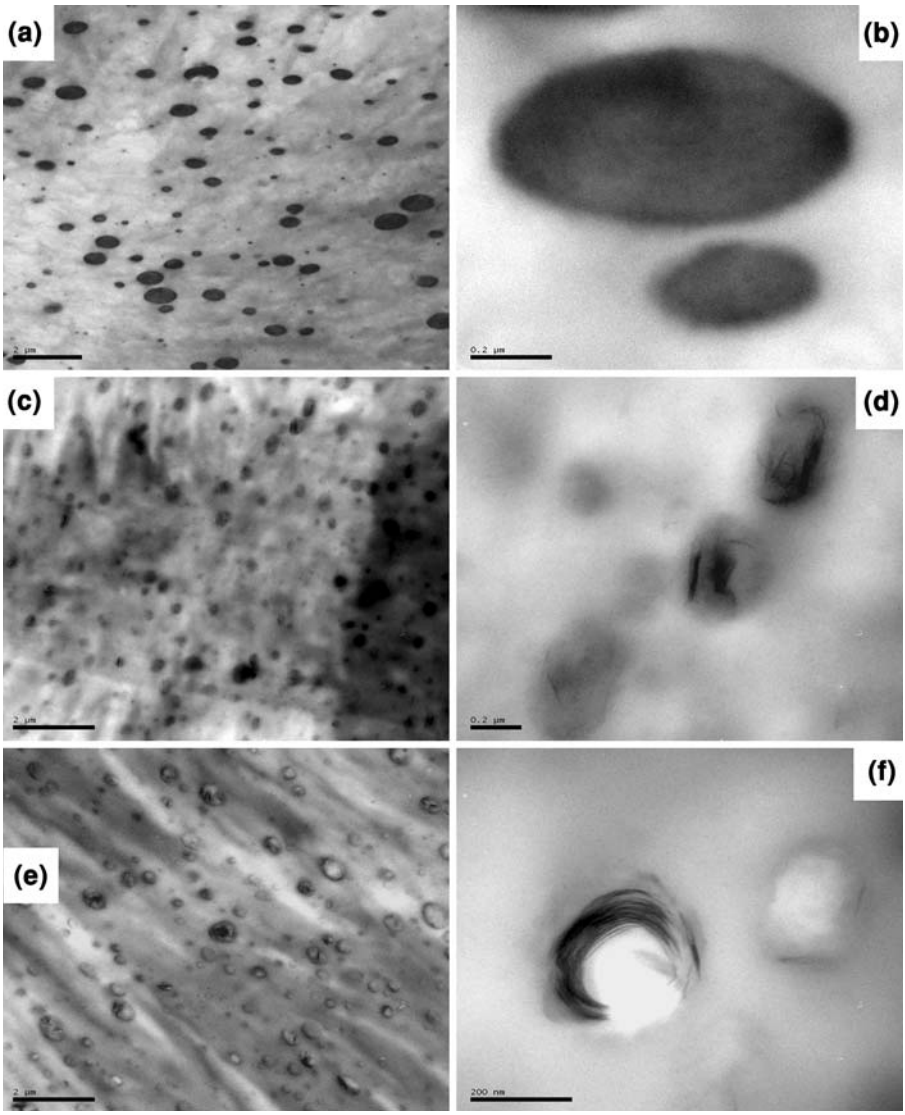

Fig. 4 TEM micrographs of **a–b** PP/SBS_{10}, **c–d** PP/$SBSn_{10}$, and **e–f** PP/$SBSne_{10}$

Ray et al. [14] suggest that the organically modified, layered silicate may act as a compatibilizer between the immiscible polymers. They pointed out three possible mechanisms of organoclay compatibilization: (1) by action of organic modifier (intercalant) miscible in both blend components, (2) by the solid–melt adsorption that results in free energy gains, and (3) by migration to the interphase and modifying the interfacial tension between the two phases. The last one seems to be confirmed by Fig. 4f.

In order to quantify the changes in domains' sizes, TEM micrographs were evaluated by means of image-analysis software. Major diameters in length (DM) and the minor (Dm)-to-major diameters ratios (Dm/DM) are presented in Figs. 5 and 6, respectively. As expected, PP/SBS blends presented the greatest values of major diameter, in the range of 0.5–0.8 μm.

The result of this interface stabilization can be attributed to PP/SBSn and PP/SBSne systems. In these blends, reductions in domains' sizes can be noticed. The rubber droplets were found to be in the range of 0.2–0.6 μm in both cases.

There are two main driving forces for reduction in domains' sizes in these systems. One is the presence of MMT, which may have modified the interface between PP and SBS phases.

In the mixture of PP/SBS, the ratio of the diameters of the particle resulted a wider morphology of an elliptical shape. With the addition of MMT this ratio of size was closer, with a morphology similar to a more spherical. With the addition of compatibilizer this ratio it is close to one and the spherical form prevails in the system (Fig. 6). Wang et al. also observed this effect in their study and state that the presence of organoclay has two competitive effects on phase morphology of nanocomposites. On one hand, organoclay acts as barriers to prevent coalescence of rubber domains and thus causes the decrease of rubber size. On the other hand, organoclay will weaken the interface adhesion and thus causes the increase of rubber size [29]. Which in our system was not observed by low polarity between the

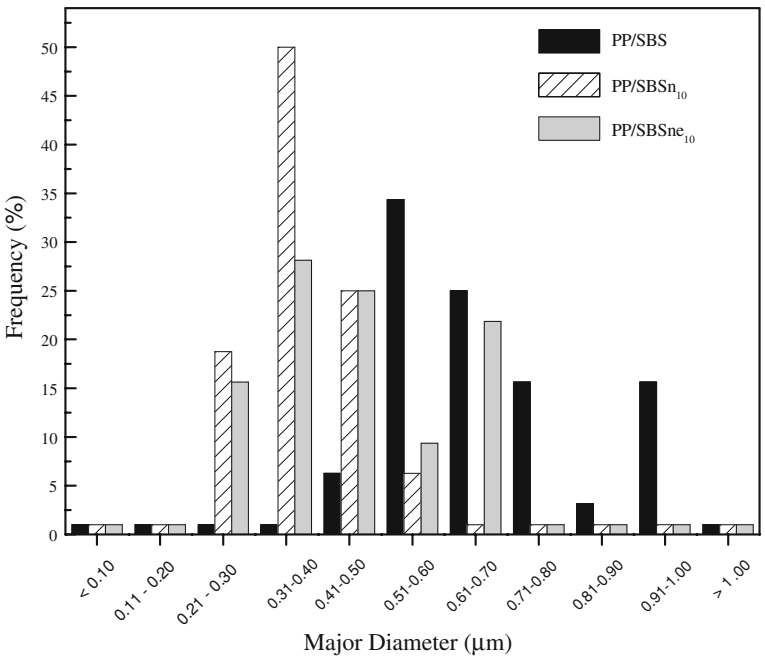

Fig. 5 Major diameters for PP/SBS blends (10 wt% of rubber)

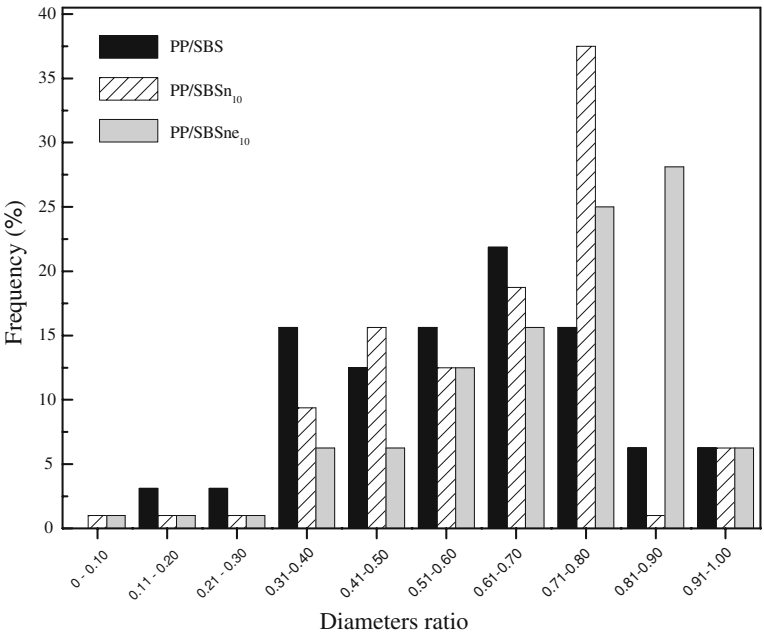

Fig. 6 Ranges of Dm/DM diameter ratios for PP/SBS blends (10 wt% of rubber)

phases, here only found the occurrence of the first effect, and with the addition of compatibilizer morphology was observed a more spherical and homogeneous.

Arroyo et al. [12], who studied epoxidized natural rubber, also noted the effect of interface with the clay resulting in the decrease of particle size, thereby leading to a more homogeneous morphology.

All these observations indicate that the clay decreases the size of the domains of rubber, the presence of compatibilizer (the clay in the interface) suggests a decrease in interfacial tension, and the domains have a more spherical shape, leading to a more homogeneous morphology that can assist in achieving improved mechanical properties.

Mechanical properties

The Table 2 presents the mechanical properties of PP/SBS systems. The tensile strength and elastic modulus were not significantly influenced by the presence of SBS or MMT; the values have remained within the standard deviation.

As expected, the addition of SBS in the PP promoted an increase in impact strength, and seems to be proportional to rubber content. The presence of MMT in the SBS also promoted the enhancement of this property. In this case, the clay may be acting as compatibilizers [34], reducing the size of the rubber phase, as shown in Fig. 4c–d.

For SBSe blends, morphology due to a more homogenous and more dispersed, with the clay at the interface, fracture resistance was greater (Fig. 4e–f) [35].

Table 2 Mechanical properties of PP/SBS systems

Sample	Tensile strength (MPa)	Elongation at break (%)	Elastic modulus (MPa)	Izod impact (J/m)
PP	33 ± 2	17 ± 5	812 ± 55	38 ± 1
PP/SBS_5	30 ± 1	65 ± 13	729 ± 23	48 ± 2
PP/SBS_{10}	26 ± 2	74 ± 10	793 ± 40	64 ± 6
PP/$SBSn_5$	27 ± 3	54 ± 1	781 ± 20	53 ± 1
PP/$SBSn_{10}$	25 ± 1	15 ± 2	771 ± 44	70 ± 4
PP/$SBSne_5$	29 ± 1	15 ± 4	824 ± 32	74 ± 3
PP/$SBSne_{10}$	26 ± 1	20 ± 5	760 ± 16	81 ± 1

PP melting (T_m) and crystallization (T_c) temperatures in the blends were only slightly influenced by the presence of SBS or MMT (Table 3). However, SBS had affected the crystallization degree of PP, decreasing its value.

In other words, the presence of SBS induced an increase in blend amorphous content, decreasing the X_c. This could be explained by means of PP/SBS interactions, which probably hindered some PP-chain segments to crystallize.

The curves of relative crystallinity as a function of time, $X_C(t)$, were calculated from DSC curves by means of Eq. 1 for PP and PP/SBS systems [36], and they are shown in Fig. 7. In this equation dQ/dt is the rate of heat flow, t_0 is the crystallization start time, t_c is the time at the end of crystallization and t is the general crystallization time. In these curves, the time to reach 50% of crystallinity is defined as the half-life time of crystallization ($t½$).

$$X_C(t) = \frac{\int_{t_0}^{t} \left(\frac{dQ}{dt}\right) dt}{\int_{t_0}^{t_c} \left(\frac{dQ}{dt}\right) dt} \quad (1)$$

$X_C(t)$ = degree of crystallinity as a function of time, t_0 = time at the crystallization start, t = crystallization time, t_c = time at the end of crystallization and dQ/dt = rate of heat flow.

Table 3 Thermal and crystallization properties of PP/SBS systems

System	T_c (°C)	T_m (°C)	X_c (%)	$t_{½}$ (min)
PP	115.5	163.9	50.1	2.6
PP/SBS_5	115.0	163.3	41.3	1.7
PP/SBS_{10}	115.6	162.5	44.1	1.7
PP/$SBSn_5$	114.7	164.5	44.3	2.2
PP/$SBSn_{10}$	114.8	164.3	46.4	2.5
PP/$SBSne_5$	114.9	163.3	45.7	2.3
PP/$SBSne_{10}$	116.1	163.4	45.8	2.2

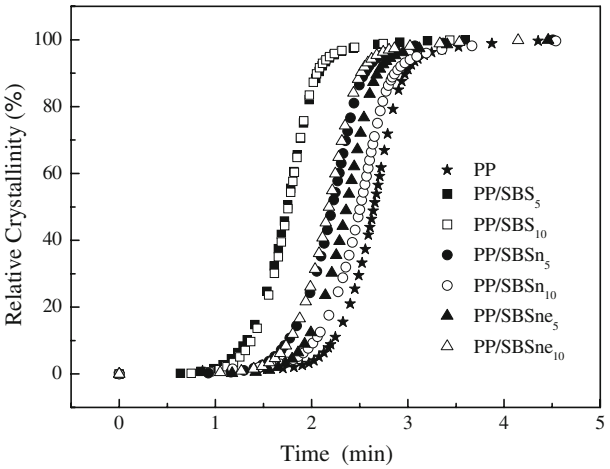

Fig. 7 Relative crystallinity as a function of time for PP/SBS blends

In the PP/SBS5 and PP/SBS10, the rubber did not influence in the extent of crystallization process, because it was not acting as a nucleation agent. The presence of SBS only had favored $t½$.

This means that the presence of SBS created an interfacial tension that introduces some energy into PP phase, inducing a faster crystallization process, and consequently a lower value of $t½$. The presence of MMT and epoxidized rubber increased half-life times, probably because the phases were more strongly associated (lower interfacial tension). This could, in turn, reduce the amount of energy introduced into PP matrix and slowing again the crystallization process.

Conclusions

Through this study, it was possible to see that the samples containing PP/SBS showed larger domains of rubber. With the addition of clay, there is a decrease of particle size, and with the addition of compatibilizer (the clay in the interface), morphology takes a spherical shape, which promotes improvement in mechanical properties. The PP crystallization process was not significantly influenced by either MMT or SBSe concerning thermal transition temperatures. On the other hand, the mixtures containing SBS crystallized faster as indicated by $t½$; the presence of MMT or SBSe slows this process down, possibly by interfacial energy reduction.

The gain in the impact strength of PP with the addition of the SBS nanocomposites was achieved by way of preparation of nanocomposites (addition of the suspension of clay in rubber in solution of SBS). The results of morphology are presented and discussed above.

Acknowledgments The authors would like to thank Petroflex Indústria e Comércio S/A, Braskem S/A, CNPq, Pronex/Fapergs, and Finep for financial support.

References

1. Hong CK, Kim MJ, Oh SH, Lee YS, Nah C (2008) Effects of polypropylene-g-(maleic anhydride/styrene) compatibilizer on mechanical and rheological properties of polypropylene/clay nanocomposites. J Ind Eng Chem 14:236
2. Denac M, Smit I, Musil V (2005) Polypropylene/talc/SEBS (SEBS-g-MA) composites. Struct Compos Part A Appl Sci Manuf Compos: Part A 36:1094–1101
3. Farahani RD, Ramazani ASA (2008) Melt preparation and investigation of properties of toughened Polyamide 66 with SEBS-g-MA and their nanocomposites. Mater Des 29:105–111
4. Paul DR, Robenson LM (2008) Polymer nanotechnology: nanocomposites. Polymer 49:3187–3204
5. Calcagno CIW, Mariani CM, Teixeira SR, Mauler RS (2007) The effect of organic modifier of the clay on morphology and crystallization properties of PET nanocomposites. Polymer 48:966–974
6. Santos KS, Liberman SA, Oviedo MAS, Mauler RS (2009) Optimization of the mechanical properties of polypropylene-based nanocomposite via the addition of a combination of organoclays. J Polym Sci: Part B Polym Phys 40:1199–1209
7. Castel CD, Bianchi O, Oviedo MA, Liberman SA, Mauler RS, Oliveira RVB (2009) The influence of interfacial agents on the morphology and viscoelasticity of PP/MMT nanocomposites. Mater Sci Eng C 29:602–606
8. Alexandre M, Dubois P (2000) Polymer-layered silicate nanocomposites: preparation, properties and uses of a new class of materials. Mater Sci Eng R Rep 28:1–63
9. Arroyo M, López-Manchado MA, Herrero B (2003) Organo-montmorillonite as substitute of carbon black in natural rubber compounds. Polymer 44:2447–2453
10. Dennis HR, Hunter DL, Chang D, Kim S, White JL, Cho JW, Paul DR (2001) Effect of melt processing conditions on the extent of exfoliation in organoclay-based nanocomposites. Polymer 42:9513
11. Zhang Z, Zhang L, Li Y, Xu H (2005) Styrene-butadiene-styrene/montmorillonite nanocomposites synthesized by anionic polymerization. J Appl Polym Sci 99:2273–2278
12. Arroyo M, López-Manchado MA, Valentin JL, Carretero J (2007) Morphology/behaviour relationship of nanocomposites based on natural rubber blends. Comp Sci Technol 67:1330
13. Sengupta R, Chakraborty S, Bandyopadhyay S, Dasgupta S, Mukhopadhyay R, Auddy K, Deuri AS (2007) A short review on rubber/clay nanocomposites with emphasis on mechanical properties. Polym Eng Sci 47:1956
14. Ray SS, Pouliot S, Bousmina M, Utracki LA (2004) Role of organically modified layered silicate as an active interfacial modifier in immiscible polystyrene/polypropylene blends. Polymer 45:8403–8413
15. Hong JS, Namkung H, Ahn KH, Lee SJ, Kim C (2006) The role of organically modified layered silicate in the breakup and coalescence of droplets in PBT/PE blends. Polymer 47:3967–3975
16. Khatua BB, Lee DJ, Kim HY, Kim JK (2004) Effect of organoclay platelets on morphology of Nylon-6 and Poly(ethylene-ran-propylene) rubber blends. Macromolecules 37:2454–2459
17. Si M, Araki T, Ade H, Kilcoyne ALD, Fisher R, Sokolov JC, Rafailovich MH (2006) Compatibilizing bulk polymer blends by using organoclays. Macromolecules 39:4793–4801
18. Halimatudahliana IH, Nasir M (2002) Morphological studies of uncompatibilized and compatibilized polystyrene/polypropylene blend. Polym Test 21:263
19. Halimatudahliana IH, Nasir M (2002) The effect of various compatibilizers on mechanical properties of polystyrene/polypropylene blend. Polym Test 21:163
20. Sung YT, Han MS, Hyun JC, Kim WN, Lee HS (2003) Rheological properties and interfacial tension of polypropylene-poly(styrene-co-acrylonitrile) blend containing compatibilizer. Polymer 44:1681–1687
21. Macaúbas PHP, Demarquette NR (2001) Morphologies and interfacial tensions of immiscible polypropylene/polystyrene blends modified with triblock copolymers. Polymer 42:2543–2554
22. Li Y, Hu S, Sheng J (2007) Evolution of phase dimensions and interfacial morphology of polypropylene/polystyrene compatibilized blends during mixing. Eur Polym J 43:561–572
23. Souza AMC, Dermaquette NR (2002) Influence of coalescence and interfacial tension on the morphology of PP/HDPE compatibilized blends. Polymer 43:3959–3967
24. Jacobi MM, Santin CK, Schuster RHV (2004) Study of the epoxidation of polydienes rubbers II. Influence of microstructure on the epoxidation of BR with performic acid. Kautsch Gummi Kunstst 57:82

25. Coutinho PA, Silva PA, Jacobi MM, Schneider LK, Barbosa RV, Cassinelli JRD, Mauler RS (2005) Processo para obtenção de material compósito em que uma nanocarga é aplicada a um polímero e material compósito resultante. Petroflex Indústria e Comércio S/A. INPI, Brazil, Patent no PI0701 345-0
26. Amash A, Zugenmaier P (2000) Morphology and properties of isotropic and oriented samples of cellulose fibre-polypropylene composites. Polymer 41:1589–1596
27. Han CD (1981) Multiphase flow in polymer processing. Academic Press, London
28. Kontopoulou M, Liu Y, Austin JR, Parent JS (2007) The dynamics of montmorillonite clay dispersion and morphology development in immiscible ethylene-propylene rubber/polypropylene blends. Polymer 48:4520–4528
29. Wang K, Wang C, Li J, Su J, Zhang Q, Du R, Fu Q (2007) Effects of clay on phase morphology and mechanical properties in polyamide 6/EPDM-g-MA/organoclay ternary nanocomposites. Polymer 48:2144
30. Li Y, Wei G, Sue H (2002) Hybrid self-assembled multilayer film formed by alternating layers of $H_4SiW_{12}O_{40}$ and 1,10—diaminodecane (DAD). J Mater Sci 37:2447–2459
31. Balakrishnan S, Start PR, Raghavan D, Hudson SD (2005) The influence of clay and elastomer concentration on the morphology and fracture energy of preformed acrylic rubber dispersed clay filled epoxy nanocomposites. Polymer 46:11255–11262
32. Kelnar I, Khunová V, Kotek J, Kaprálková L (2007) Effect of clay treatment on structure and mechanical behaviour of elastomer – containing polyamide 6 nanocomposite. Polymer 48:5332–5339
33. Contreras V, Cafiero M, Da Silva S, Rosales C, Perera R, Matos M (2006) Characterization and tensile properties of ternary blends with PA-6 nanocomposites. Polym Eng Sci 46:1111–1120
34. Wang Y, Zhang Q, Fu Q (2003) Compatibilization of immiscible poly(propylene)/polystyrene blends using clay. Macromol Rapid Commun 24:231
35. Zebarjad SM, Lazzeri A, Bagheri R, Reihani SMS, Frounch M (2003) Fracture mechanism under dynamic loading of elastomer-modified polypropylene. Mater Lett 57:2733–2741
36. Jain S, Goossens H, Duin MV, Lemstra P (2005) Effect of in situ prepared silica nano-particles on non-isothermal crystallization of polypropylene. Polymer 46:8805–8818